

# Device for monitoring the temperature and diameter of an extended cylindrical object in the high-temperature manufacturing process

**Alexander Tomashuk**

Igor Sikorsky Kyiv Polytechnic Institute, Kyiv, Ukraine

E-mail: tomashuk.alexander@gmail.com

**Abstract.** The paper describes a method and a device for monitoring the temperature and diameter of an extended cylindrical object in the high-temperature manufacturing process, such as hot rolling, die-less drawing, etc. The proposed integrated approach based on optical phenomena, such as Fresnel diffraction, makes it possible to monitor parameters of the heated object both on a focused and a defocused image with high measurement accuracy.

## 1. Introduction

In order to improve the quality of an extended cylindrical product (metal tubes and wires, chemical fibers, optical fibers, etc.), it is necessary to monitor its parameters in the manufacturing process in real time.

In order to monitor the geometrical parameters of the products obtained by traditional rolling or drawing a large number of works [1-3] were published.

In the process of some modern approaches, such as die-less drawing (pulling the thread out of the material melt), it is necessary to monitor both its basic geometrical parameters and the surface temperature simultaneously [4-6].

The proposed method of measuring and monitoring the diameter and temperature of an extended cylindrical object is based on optical phenomena. The method allows to measure the parameters of the object on its defocused image. The method can also be applied in microscopic studies of other objects, which have a physical size smaller than optical resolution of a microscope.

## 2. Description of the proposed method

### 2.1. Device design

The design of the device and the scheme of obtaining the shadow image of the object and the Fresnel diffraction pattern, which was formed as a result of deviations from the laws of geometric optics, are shown in figure 1.

The design of the experimental device as a point source of illumination was used the design of a powerful LED and an adjustable slot. With a decrease in the physical dimensions of the point source, the diffraction pattern blur decreases. This increases the resolution of the diffraction pattern when projecting onto a remote screen [7].



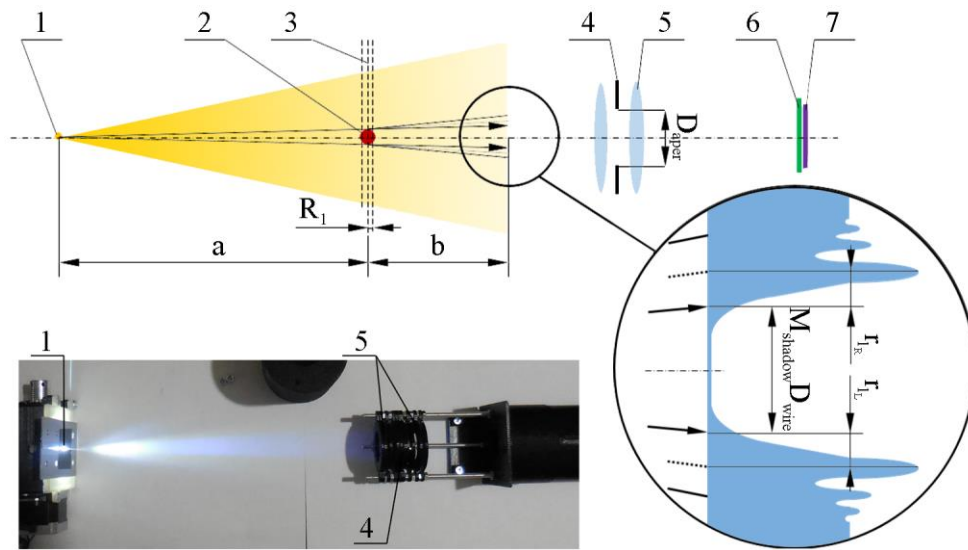


**Figure 1.** The design of the device and the scheme for obtaining the image of the shadow of the object: 1 - a point source of illumination; 2 - extended cylindrical object; 3 - the plane of focusing of the receiving device rays of the optical system; 4 - aperture; 5 - lens (achromatic doublet); 6 - narrowband light filter; 7 - photoelectric cells matrix;  $a$  - the distance between the point source of illumination and the object;  $b$  - the distance between the object and the projection;  $R_1$  and  $R_2$  - the depth of field, front and rear, respectively;  $D_{aper}$  - the diameter of the aperture;  $M_{shadow}$  - scale of object shadow image;  $D_{wire}$  - the object diameter;  $r_{L_R}$  and  $r_{L_L}$  - the radii of the first Fresnel zones on both sides of the edges of the object shadow image, right and left, respectively.

## 2.2. Measurement of the object diameter

2.2.1. *The scale of the object image.* Scale of the object shadow image  $M_{shadow}$  is expressed as follows:

$$M_{shadow} = (a + b) / a. \quad (1)$$

Further, when the object is removed from the focal length and is approached to the optical system of the receiving device, the distance  $b$  takes on negative values. Thus, for this case, the scale of the object shadow  $M_{shadow}$  takes on a value  $M_{shadow} < 1$ , which later became apparent from the results.

On a focused image, the distance  $b$  is equal to the depth of the front sharply depicted space, that is  $b_0 = R_1$ .

Optical zoom  $M_{OS}$  is expressed in the following equation:

$$M_{OS} = (n_1 f_2) / (n_2 f_1), \quad (2)$$

where  $n_1$  and  $n_2$  = the refractive indices of the environment, in the space of the object and the image, respectively;  $f_1$  и  $f_2$  = focal lengths, front and rear, respectively.

2.2.2. *Measurement of the diameter of the object.* Figure 2 shows the basics of the known method [3].

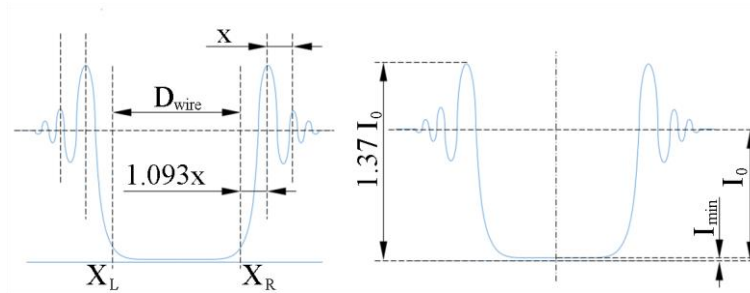


**Figure 2.** Determination of the diameter of a cylindrical object using a known diffraction method:  $x$  - a segment equal to the distance between two centers of diffraction extremes;  $X_L$  and  $X_R$  - coordinates of the begin and end of the image of the shadow of the object;  $I_0$  - brightness of the background image;  $I_{min}$  - minimum brightness, which depends on the quality of the optical system.

If the distance  $a_0$  for the stationary case (the distance from the light source to the focal point) is known, and the object is at the focal point, then the radiuses  $r_{I_L}$  and  $r_{I_R}$  are known ( $b = R_I$ ,  $r_{I_L} = r_{I_R}$ ).

The radius of the Fresnel zone  $m$  for the wavelength  $\lambda$  is determined by the formula:

$$r_m = \left( \frac{ab}{a+b} \lambda m \right)^{1/2}. \quad (3)$$

For resolution of the diffraction pattern using the optical system of the device, it is necessary that the condition  $r_I > y_{min}$  is met, where  $y_{min}$  is the minimum resolution of the optical system, which is determined, in the simplest case, by Rayleigh criterion (for a thin lens), or by experimentally determining the modulation transfer function [8].

When the object is moved from the focal length of the optical system towards the source of illumination, the values of the radiuses  $r_{I_L}$  and  $r_{I_R}$  increase, which indicate an increase in scale  $M_{shadow}$ .

When measurements are made using only one device (one axis) without prior calibration it is impossible to establish the exact distance  $b$ . Therefore, it is necessary to create an array of values that shows the ratio of the radius to scale values  $r_I(M_{shadow})$ . Such an array can be composed using a cyclic procedure, in which  $a = a_0 - i$  and  $b = b_0 + i$ , where  $i$  is the step by which the shift in distance occurs.

The diameter of a cylindrical object is determined by the equation:

$$D_{wire} = l_{px} (X_R - X_L) / (M_{shadow} M_{OS} \Delta_{scale}(b)), \quad (4)$$

where  $l_{px}$  is the physical size of the photoelectric cell of the matrix,  $\Delta_{scale}(b)$  is the deviation of the scale, which is determined using the measured distance  $b$ .

### 2.3. Object temperature measurement

Temperature measurement can be performed using optical pyrometry methods, which are based on a black body model (brightness pyrometry) [9], or using calibration of the device with a reference product ( $I(T)$  ratio).

**2.3.1. Object temperature measurement.** Figure 3 shows the distribution of the image brightness, which is formed by two sources - the point source of illumination and the heated surface of the object.

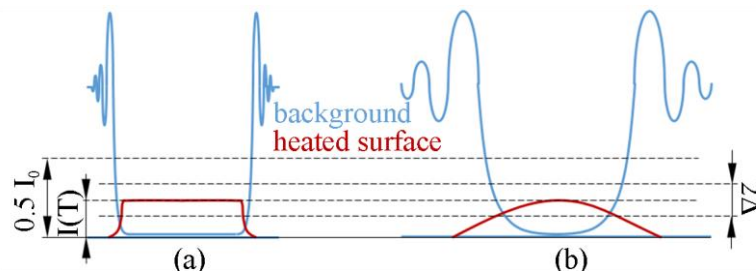


**Figure 3.** The distribution of brightness in the horizontal profile of the heated object image: (a) focused image; (b) defocused image.

As the image of the diffraction pattern may be disturbed due to the high brightness of the object, the solution may be the use of a certain brightness threshold value.

If there is an increase in the brightness of the image of the object (temperature increase), as well as overcoming the threshold brightness value, the scanning speed can be increased (the exposure time is decrease) to the required brightness value on the sensor.

In this case, the brightness of the light source must be increased to obtain the required brightness of the background image in the ratio:

$$I_0 / (I(T) \pm \Delta) \approx \text{const at } I_{\min} < I(T) \pm \Delta < 0.5 I_0, \quad (5)$$

where  $T$  is the surface temperature of the object,  $\Delta$  is the selected brightness range for the measured signal.

As it can be seen from figure 3, in order to measure the temperature of an object, the center point  $(x, y)$  in its image should be used.

**2.3.2. Measurement of the temperature of the object in a defocused image.** To measure the temperature of a heated object in a defocused image, it is necessary to understand how the energy distribution takes place when constructing such an image.

In theory, it can be described with the help of a Gaussian beam, and in practice it can be determined experimentally by determining the spatial frequency (diameter) of a test-object as a function of its displacement along the optical axis by a specific distance from the beam focusing plane by the optical system.

In order to be able to assess whether it is possible to measure the temperature of an object and with what accuracy, it is necessary to determine how far the object has moved from the focal plane. It is possible to evaluate whether it is possible to measure the temperature of an object and with what accuracy having determined how far  $b$  object has deflected using the following equation:

$$b = M_{\text{shadow}} r_l^2 / \lambda. \quad (6)$$

For example, for a wire (NiCr alloy) with a diameter  $D_{wire} = 497 \mu m$  and the optical system of our experimental device, the allowable distance was  $\pm 10D_{wire}$ , which is shown in figure 4 (the light source is turned off). For wire with a diameter  $D_{wire} = 50 \mu m$ , the allowable distance was  $\pm 20D_{wire}$ .

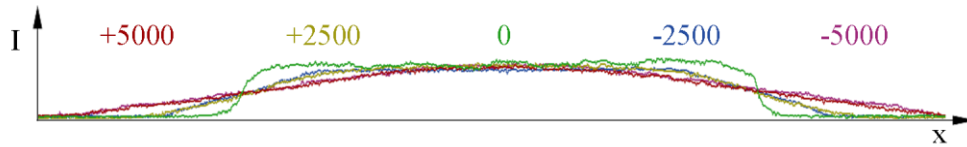


**Figure 4.** The brightness distribution in the image of a heated wire with a diameter of  $497 \mu m$ , when it is moved from the plane of focusing the rays by the optical system for some distance: where '+' is the defocused image of the object when it approaches the source of light at a certain distance (in  $\mu m$ ); '-' is defocused image of the object, when it approaches the optical system at a certain distance.

### 3. Results and discussion

The parameters of the experimental device that were used to obtain the results: the width of the slot  $w_{slot} = 120 \mu m$ ;  $a_0 = 235 mm$ ;  $\lambda = 0.532 \mu m$ ;  $y_{min} = 2.7 \mu m$ ;  $M_{OS} = 3.5$ ;  $R_2 \approx R_l = 17 \mu m$ ;  $l_{px} = 3.03 \mu m$ .

Algorithm of Section 2.2.2 and the results of the determination  $r_l(M_{shadow})$  are shown in Figure 5.

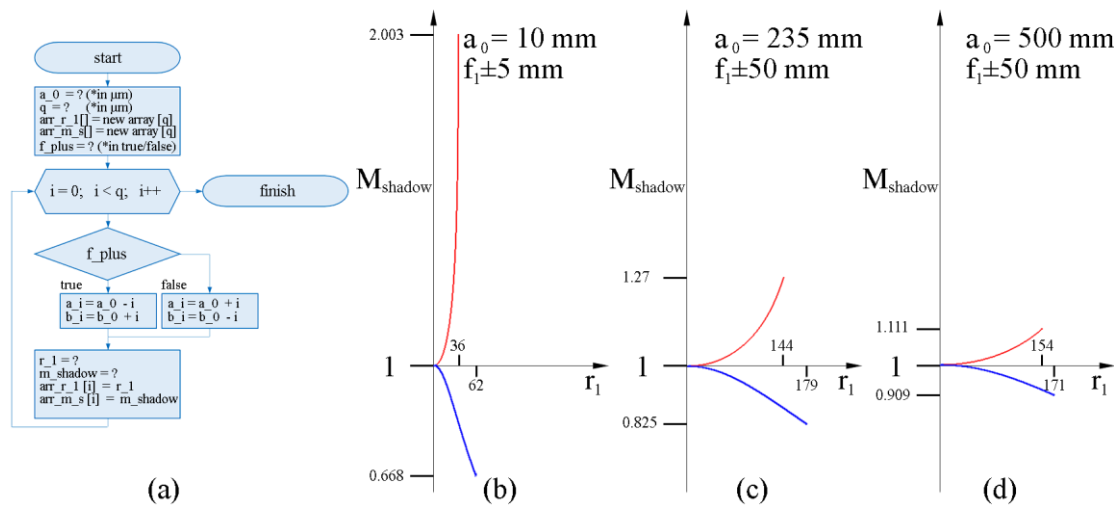


**Figure 5.** The algorithm of the cyclic procedure and the determination results  $r_l(M_{shadow})$ : (a) algorithm; (b), (c), (d) results; (b)  $a_0 = 10 mm$ ; (c)  $a_0 = 235 mm$ ; (d)  $a_0 = 500 mm$ .

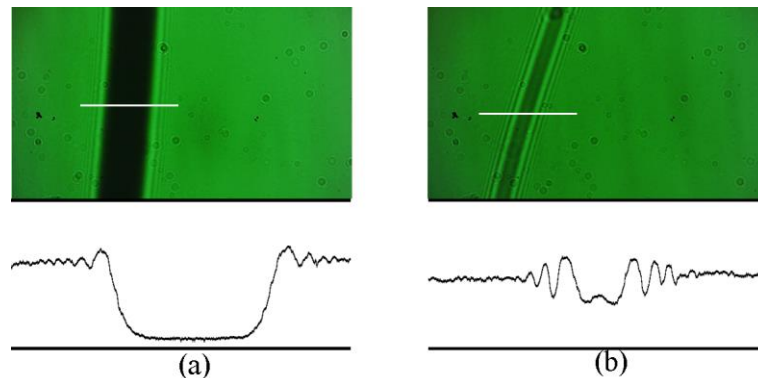
Figure 5 shows that the greater the distance  $a$  between the light source and the focal point is, the smaller deviations the sample of the values of the scale of the image of the shadow of the object has.

Figure 6 shows the images that were obtained by the experimental device.

For our device, the standard deviation of the measured wire diameter ( $D_{wire} = 200 \mu m$ ) was  $\sigma_{D_{wire}} = 5 \mu m$ , respectively,  $\Delta_{D_{wire}} = \pm 5 \mu m$ .

For our device, the standard deviation of the measured temperature  $T_{wire}(x, y) = 520^{\circ}\text{C}$  of the heated wire was  $\sigma_{T_{wire}} = 7^{\circ}\text{C}$ , respectively,  $\Delta_{T_{wire}} = \pm 7^{\circ}\text{C}$ .

The consideration of additional factors and errors, special image processing algorithms [10], as well as the use of industrial cameras with a high signal-to-noise ratio, makes it possible to increase the accuracy of the measurements of both parameters, which would be characterized by smaller deviations.



**Figure 6.** Images of objects and the distribution of brightness in a horizontal profile: (a) heated wire with a diameter of  $200\ \mu\text{m}$ ; (b) carbon fiber with a diameter of  $10\ \mu\text{m}$ .

#### 4. Conclusions

A method and device for simultaneous measuring and monitoring two parameters of a heated extended cylindrical object, such as temperature and diameter, in the high-temperature manufacturing process, was proposed. The method is based on optical phenomena that allow high-precision measurements compared with most methods used in machine vision systems.

#### References

- [1] Khodier S A 2004 *Opt. & Las. Technol.* **36** 63-7
- [2] Lemeshko Ya A and Chuguy Yu V 2005 *Avtometriya* **6** 3-12
- [3] Fedorov M E 2015 *IOP Conf. Ser.: Mater. Sci. Eng.* **81** 012074
- [4] He Y, Liu X, Qin F and Xie J 2012 *Int. J. Miner. Metall. Mater.* **19** 615-21
- [5] Supriadi S, Furushima T and Manabe K 2012 *Mater. Trans.* **53** 862-9
- [6] Milenin A, Kustra P, Du P, Furusawa S and Furushima T 2018 *Proc. Manuf.* **15** 302-10
- [7] Tilikin I N, Shelkovenko T A, Pikuz S A and Hammer D A 2013 *Opt. and Spectr.* **115** 147-56
- [8] Leung C and Donnelly T D 2017 *Am. J. Phys.* **85** 429-38
- [9] Gulyaev I and Dolmatov A 2018 *Int. J. Heat Mass Tran.* **116** 1016-25
- [10] Porev V and Tomashuk A 2017 *Tech. Diagn. Non-Destr. Test.* **4** 52-5